Langmuir Article

pubs.acs.org/Langmuir

Electrosteric Enhanced Stability of Functional Sub-10 nm Cerium and Iron Oxide Particles in Cell Culture Medium

B. Chanteau,[†] J. Fresnais,[‡] and J.-F. Berret*,[†]

[†]*Matière et Systèmes Complexes, UMR 7057 CNRS Université Denis Diderot Paris-VII, Bâtiment Condorcet, 10 rue Alice Domon et Léonie Duquet, F-75205 Paris, France, and* [‡]*UPMC Université Paris VI, Laboratoire de Physico-chimie des Electrolytes, Colloides et Sciences Analytiques UMR 7195 CNRS, 4 place Jussieu, F-75252 Paris, France*

Received March 8, 2009. Revised Manuscript Received May 7, 2009

Applications of nanoparticles in biology require that the nanoparticles remain stable in solutions containing high concentrations of proteins and salts, as well as in cell culture media. In this work, we developed simple protocols for the coating of sub-10 nm nanoparticles and evaluated the colloidal stability of dispersions in various environments. Ligands (citric acid), oligomers [phosphonate-terminated poly(ethylene oxide)], and polymers [poly(acrylic acid)] were used as nanometer-thick adlayers for cerium (CeO_2) and iron (γ-Fe_2O_3) oxide nanoparticles. The organic functionalities were adsorbed on the particle surfaces via physical (electrostatic) forces. Stability assays at high ionic strengths and in cell culture media were performed by static and dynamic light scattering. Of the three coatings examined, we found that only poly(acrylic acid) fully preserved the dispersion stability over the long term (longer than weeks). The improved stability was explained by the multipoint attachments of the chains onto the particle surface and by the adlayer-mediated electrosteric interactions. These results suggest that anionically charged polymers represent an effective alternative to conventional coating agents.

I. Introduction

Inorganic nanoparticles (NP) made from gold, metal oxides, or semiconductors are emerging as the central constituents of future nanotechnological developments. Interest stems from the combination of complementary attributes, such as a size in the nanometer range and unique physical features, including high reactivity, magnetic, or optical properties. In biomedicine, inorganic nanoparticles have attracted interest with respect to applications such as magnetic separation, biosensor devices, diagnostics, imaging, and therapeutics.[1] Nanomaterials also possess very high specific surfaces (a few hundred square meters per gram of 10 nm particles) which may enhance their chemical reactivity with respect to living organisms. As compared to conventional chemicals, the risk assessment of nanomaterials toward human health has not been fully appreciated. Issues dealing with the impacts, fate, and toxicity of nanoparticles on the environment have become the focus of much recent research, and in particular of in vitro toxicology experiments.[2−12] The objective of toxicology assays, such as MTT, neutral red, or WST1, is the quantitative determination of the viability of living cells that were incubated with nanomaterials.[13] Brunner et al. submitted rodent fibroblasts to various industrially important particles and measured the cell responses in terms of metabolic activity and cell proliferation.[8] Their results revealed that most uncoated particles were cytotoxic. Limbach et al. focused on the transport and uptake of cerium oxide NPs into human lung fibroblasts and found that the size of the particles was the decisive criterion.[4] In these studies and in others,[2,5,7,9,14−16] it was also recognized that the physicochemical characteristics of the particles (and not only the nature of their atomistic constituents) played a crucial role in cellular uptake. The chemistry of the interfaces between nanocrystal and solvent was also anticipated to be a key feature of the cell−NP interactions. Should the particle surfaces be charged or neutral, should they be tethered with polymers, oligomers, or low-molecular weight molecules, or should the particles be aggregated into large clusters, the interactions toward cells would be drastically different.[2−4,6−10,12,17]

In this work, we emphasize a feature that was not systematically addressed in toxicology studies of nanomaterials, their

*To whom correspondence should be addressed. E-mail: jean-francois.berret@univ-paris-diderot.fr.

(1) Ferrari, M. *Nat. Rev. Cancer* **2005**, *5*(3), 161–171.
(2) Chastellain, M.; Petri, A.; Hofmann, H. *J. Colloid Interface Sci.* **2004**, *278*(2), 353–360.
(3) Derfus, A. M.; Chan, W. C. W.; Bhatia, S. N. *Nano Lett.* **2004**, *4*(1), 11–18.
(4) Limbach, L. K.; Li, Y.; Grass, R. N.; Brunner, T. J.; Hintermann, M. A.; Muller, M.; Gunther, D.; Stark, W. J. *Environ. Sci. Technol.* **2005**, *39*(23), 9370–9376.
(5) Oberdorster, G.; Maynard, A.; Donaldson, K.; Castranova, V.; Fitzpatrick, J.; Ausman, K.; Carter, J.; Karn, B.; Kreyling, W.; Lai, D.; Olin, S.; Monteiro-Riviere, N.; Warheit, D.; Yang, H. *Part. Fibre Toxicol.* **2005**, *2*(1), 8.
(6) Rothen-Rutishauser, B. M.; Schurch, S.; Haenni, B.; Kapp, N.; Gehr, P. *Environ. Sci. Technol.* **2006**, *40*(14), 4353–4359.
(7) Auffan, M.; Decome, L.; Rose, J.; Orsiere, T.; DeMeo, M.; Briois, V.; Chaneac, C.; Olivi, L.; Berge-Lefranc, J.-L.; Botta, A.; Wiesner, M. R.; Bottero, J.-Y. *Environ. Sci. Technol.* **2006**, *40*(14), 4367–4373.
(8) Brunner, T. J.; Wick, P.; Manser, P.; Spohn, P.; Grass, R. N.; Limbach, L. K.; Bruinink, A.; Stark, W. J. *Environ. Sci. Technol.* **2006**, *40*(14), 4374–4381.
(9) Lorenz, M. R.; Holzapfel, V.; Musyanovych, A.; Nothelfer, K.; Walther, P.; Frank, H.; Landfester, K.; Schrezenmeier, H.; Mailander, V. *Biomaterials* **2006**, *27*(14), 2820–2828.
(10) Williams, D.; Ehrman, S.; Pulliam Holoman, T. *J. Nanobiotechnol.* **2006**, *4*(1), 3.
(11) Teeguarden, J. G.; Hinderliter, P. M.; Orr, G.; Thrall, B. D.; Pounds, J. G. *Toxicol. Sci.* **2007**, *97*(2), 614.
(12) Diaz, B.; Sanchez-Espinel, C.; Arruebo, M.; Faro, J.; de Miguel, E.; Magadan, S.; Yague, C.; Fernandez-Pacheco, R.; Ibarra, M. R.; Santamaria, J.; Gonzalez-Fernandez, A. *Small* **2008**, *4*(11), 2025–2034.
(13) Berridge, M. V.; Herst, P. M.; Tan, A. S. *Biotechnol. Annu. Rev.* **2005**, *11*, 127–152.
(14) Boldt, K.; Bruns, O. T.; Gaponik, N.; Eychmuller, A. *J. Phys. Chem. B* **2006**, *110*(5), 1959–1963.
(15) Lattuada, M.; Hatton, T. A. *Langmuir* **2007**, *23*(4), 2158–2168.
(16) Petri-Fink, A.; Steitz, B.; Finka, A.; Salaklang, J.; Hofmann, H. *Eur. J. Pharm. Biopharm.* **2008**, *68*(1), 129–137.
(17) Limbach, L. K.; Bereiter, R.; Mueller, E.; Krebs, R.; Gaelli, R.; Stark, W. J. *Environ. Sci. Technol.* **2008**, *42*(15), 5828–5833.

colloidal stability in a cellular culture medium. In a certain number of reports, it was found that in culture media particles aggregated almost systematically, yielding the formation of large clusters and sedimentation.[7,10,12,14,16,18,19] In addition, the aggregation was irreversible and in some cases corresponded to the loss of the physical size-related attributes.[10] Other scenarios have shown that in serum-rich media, particles were covered by proteins such as immunoglobulins, yielding large core−corona hybrid structures.[20] In this work, we have investigated the role of the coating on the colloidal stability of cerium (CeO_2) and iron oxide (γ-Fe_2O_3) nanoparticles in complex environments. The particles have been dispersed in the culture medium that is employed for the growth of eukaryotic cells (Dulbecco's modified Eagle's medium supplemented with calf serum and antibiotics). Three different coatings using small organic molecules and macromolecules were produced through simple protocols and physical (electrostatic) interactions with the particles.[21] Here, we demonstrate that electrosteric (a combination of electrostatic and steric repulsions[22]) coating can be robust and efficient for stabilizing nanoparticles.

II. Experimental Section

1. Nanoparticles. *Cerium Oxide Nanoparticles (nanoceria).* The cerium oxide nanoparticles (bulk mass density[23] ρ = 7.1 g/cm^3) were synthesized in a nitric acid solution at pH 1.4 by thermohydrolysis of a cerium(IV) nitrate salt solution at high temperatures. The thermohydrolysis resulted in the homogeneous precipitation of cerium oxide nanoparticles.[24] The size of the particles was controlled by addition of hydroxide ions during the procedure. An image of transmission electron microscopy (TEM) obtained from a dispersion at 0.2 wt % is illustrated in Figure 1a. It shows that the nanoceria consisted of isotropic agglomerates of ~2 nm crystallites with faceted morphologies. An image analysis of the TEM data allowed us to derive the size distribution of the NPs. A log-normal function with a median diameter D_0 of 7.0 nm and a polydispersity s of 0.15 accounts well for the size distribution.[25] The polydispersity was defined as the ratio between the standard deviation and the average diameter. Wide-angle X-ray scattering confirmed the crystalline fluorite face-centered cubic structure of the nanocrystallites (see part SI.1 of the Supporting Information). Using static and dynamic light scattering, the molecular weight (M_W) and the hydrodynamic diameter (D_H) of the particles under acidic conditions were determined to be 330 kg/mol and 9 nm, respectively (Table 1).[26] As synthesized, the cerium oxide nanosols were stabilized by electrostatic repulsive interactions. An increase in pH or ionic strength produced, however, an instantaneous and irreversible aggregation of the particles, and ultimately a destabilization of the sols.[23,24]

Iron Oxide Nanoparticles (maghemite). The iron oxide nanoparticles (bulk mass density ρ = 5100 kg/m^3) were synthesized according to the Massart method[27] by (i) alkaline coprecipitation of iron(II) and iron(III) salts, (ii) oxidation of the magnetite (Fe_3O_4) into maghemite (γ-Fe_2O_3) NPs, and (iii) size sorting by subsequent phase separations.[27,28] At the end of the process, the particles were at concentrations (c) of ~10 wt % and under acidic conditions (pH 1.8). As for the nanoceria, the particles were positively charged, with nitrate counterions adsorbed on their surfaces. The resulting electrostatic repulsion between nanocolloids also ensured a remarkable colloidal stability of the dispersions, typically over several years. The size distributions as determined from TEM measurements (Figure 1b,c) could be represented by a log-normal function, with median diameter D_0 and polydispersity s.[29] For this study, two maghemite batches of different particle sizes were synthesized, one under acidic conditions with a D_0 of 7.1 nm (batch termed "acidic" in Table 1) and one coated with citrate counterions with a D_0 of 8.5 nm (batch termed "citrated"). For these systems, the polydispersity was estimated to be 0.26 and 0.29, respectively. The magnetic nanosols were further characterized by electron microdiffraction, vibrating

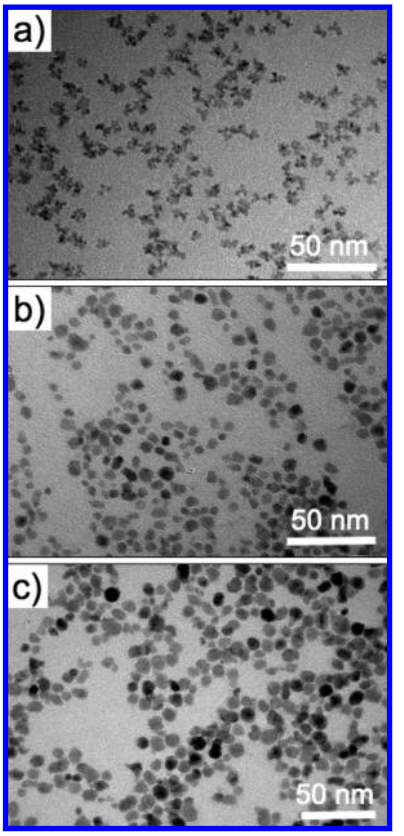

Figure 1. Transmission electron microscopy images (120000× magnification) of the nanoparticles investigated in this work: (a) cerium oxide (CeO_2), (b) iron oxide (γ-Fe_2O_3) under acidic conditions, and (c) iron oxide (γ-Fe_2O_3) coated with citrate counterions at neutral pH. Image analysis of the TEM data allowed us to derive the size distribution of the different nanocrystals (Table 1).

Table 1. Median Diameters (D_0), Polydispersities (s), Molecular Weights (M_W), and Hydrodynamic Diameters (D_H) of the Bare Nanoparticles Studied in This Work[a]

nanoparticle	D_0 (nm)	s	M_W (kg/mol)	D_H (nm)
CeO_2	7.0	0.15	330	9
γ-Fe_2O_3 (acidic)	7.1	0.26	1400	14
γ-Fe_2O_3 (citrated)	8.5	0.29	3000	23

[a] The size distributions of the particles were assumed to be log-normal for the three batches.

(18) Liu, Y. L.; Shipton, M. K.; Ryan, J.; Kaufman, E. D.; Franzen, S.; Feldheim, D. L. *Anal. Chem.* **2007**, *79*(6), 2221–2229.
(19) Allouni, Z. E.; Cimpan, M. R.; Hol, P. J.; Skodvin, T.; Gjerdet, N. R. *Colloids Surf., B* **2009**, *68*(1), 83–87.
(20) Cedervall, T.; Lynch, I.; Lindman, S.; Berggard, T.; Thulin, E.; Nilsson, H.; Dawson, K. A.; Linse, S. *Proc. Natl. Acad. Sci. U.S.A.* **2007**, *104*(7), 2050–2055.
(21) Berret, J.-F. *J. Chem. Phys.* **2005**, *123*(16), 164703.
(22) Lewis, J. A. *J. Am. Ceram. Soc.* **2000**, *83*, 2341–2359.
(23) Spalla, O.; Cabane, B. *Colloid Polym. Sci.* **1993**, *271*, 357–371.
(24) Sehgal, A.; Lalatonne, Y.; Berret, J.-F.; Morvan, M. *Langmuir* **2005**, *21*(20), 9359–9364.
(25) Qi, L.; Chapel, J. P.; Castaing, J. C.; Fresnais, J.; Berret, J.-F. *Soft Matter* **2008**, *4*(3), 577–585.
(26) Qi, L.; Sehgal, A.; Castaing, J. C.; Chapel, J. P.; Fresnais, J.; Berret, J. F.; Cousin, F. *ACS Nano* **2008**, *2*(5), 879–888.
(27) Massart, R.; Dubois, E.; Cabuil, V.; Hasmonay, E. *J. Magn. Magn. Mater.* **1995**, *149*(1−2), 1–5.
(28) Bee, A.; Massart, R.; Neveu, S. *J. Magn. Magn. Mater.* **1995**, *149*(1−2), 6–9.
(29) Berret, J.-F.; Sandre, O.; Mauger, A. *Langmuir* **2007**, *23*(6), 2993–2999.

Table 2. Light Scattering Data Found for the Coated Nanoparticles Dispersed in Deionized Water[a]

coated NP	$R(c)/c$ (cm^{-1})	D_H (nm)	$2h$ (nm)
Cit−CeO_2	0.091	9	< 1
PPEG−CeO_2	0.076	12	3
PAA_{2K}−CeO_2	0.150	13	4
Cit−γ-Fe_2O_3[b]	0.70	23	< 1
PPEG−γ-Fe_2O_3[c]	0.51	17	3
PAA_{2K}−γ-Fe_2O_3[c]	0.60	19	5
PAA_{5K}−γ-Fe_2O_3[c]	0.71	22	8

[a] $R(c)$ denotes the excess Rayleigh ratio, D_H the hydrodynamic diameter, and $2h$ the increase in diameter due to the organic adlayer. In the concentration range explored (10^{-3}−10^{-1} wt %), the Rayleigh ratios of the dispersions were found to vary linearly with concentration, with slopes indicated in the first column. [b] Batch of maghemite particles coated during the synthesis and termed citrated in Table 1. [c] Batch of uncoated maghemite particles and termed acidic in Table 1.

sample magnetometry, magnetic sedimentation, and light scattering[29] (see the Supporting Information for details). For iron oxide NPs, it should be noted that the hydrodynamic sizes appeared to be larger than the median diameters found by TEM. These differences were attributed to two effects:[29] the slight anisotropy of the γ-Fe_2O_3 particles (aspect ratio of 1.2) and the fact that light scattering is more sensitive to the large particles of a distribution.[30]

2. Chemicals and Coating. For this work, we have developed different types of coating based on the electrostatic adsorption of the organic adlayer on the particles. Ligands (citric acid),[24] oligomers [phosphonate-terminated poly(ethylene oxide)],[26] and polymers [poly(acrylic acid)][24] were used alternatively.

Citric Acid. Citric acid is a weak triacid with a molecular weight M_W of 192.1 g/mol, which has three acidity constants: $pK_{a1} = 3.1$, $pK_{a2} = 4.8$, and $pK_{a3} = 6.4$. Complexation of the surface charges with citric acid (Sigma Aldrich) was performed during the synthesis. It allowed us to reverse the surface charge of the particles from cationic at low pH to anionic at high pH, through an ionization of the carboxyl groups. At pH 8, the particles were stabilized by electrostatic interactions mediated by the anionically charged ligands.[24] As a ligand, citrate ions were characterized by adsorption isotherms; i.e., the adsorbed species were in equilibrium with free citrate molecules dispersed in the bulk. The concentration of free citrates in the bulk was kept at 8 mM,[23,31,32] both in water and in culture medium. It should be noted that the hydrodynamic diameters of the bare and citrate-coated particles were identical within experimental accuracy, indicating a layer thickness of < 1 nm (Table 2). The citrate-coated particles are denoted Cit−CeO_2 and Cit−γ-Fe_2O_3 herein.

Phosphonate-Terminated PEG (PPEG). Poly(oxy-1,2-ethanediyl) α-(3-phosphonopropyl) ω-hydroxyl, abbreviated PPEG in the following, is an oligomer of the phosphonated poly(oxyalkene) class that was produced by Rhodia Chemicals for the purpose of coating. PPEG titration curves have shown the presence of two pK_a values ($pK_{a1} = 2.7$ and $pK_{a2} = 7.8$) associated with the ionization of the phosphonate group. Mixed solutions of nanoparticles and PPEG were prepared by simple mixing of dilute solutions prepared at pH 2.[26] This ensured that no aggregation of nanoparticles occurred due to a pH or salinity gap. The relative amount of each component was monitored by the volume ratio between the NP and oligomer stock solutions. This mixing ratio was chosen so that there was a large excess of oligomers per particle.

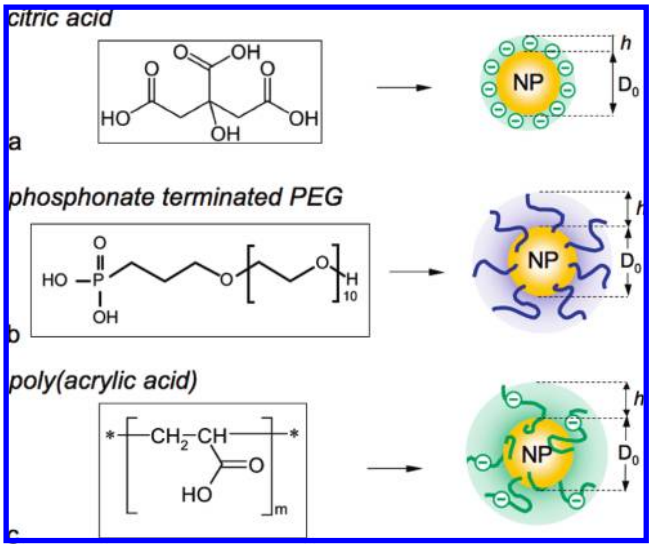

Figure 2. Schematic description of the three different coatings developed in this study. The organic functionalities were adsorbed on the particle surfaces through electrostatic complexation. In cases a and c, the coating was anionic, whereas in case b, it was neutral. D_0 denotes the diameter of the particles as derived from TEM measurements. The thickness of the organic adlayers, noted h, was derived from dynamic light scattering. h was on the order of a few angstroms for the citric acid and a few nanometers for the others (see Table 2).

Ammonium hydroxide (NH_4OH) was used to adjust the pH of PPEG−CeO_2 and PPEG−γ-Fe_2O_3 dispersions in the range from 1.5 to 10. In this range, the hydrodynamic diameter was found to be constant and at a value that exceeded that of the bare NPs by $2h = 3$ nm, h being the adlayer thickness (Table 2). A recent study of PPEG-coated nanoceria by light and neutron scattering revealed an average of 270 PPEG oligomers per particle for the dialyzed dispersions.[26] This value corresponds to a density of adsorbed species of 1 nm^{-2}. Thanks to the external PEG terminus, the particles were found to be neutral, as revealed by the very small values of electrophoretic mobility.

Poly(acrylic acid). Over the past several years, poly(acrylic acid) (PAA) was frequently used as a coating agent of inorganic particles.[15,17,24,25,33−35] Poly(sodium acrylate), the salt form of PAA with molecular weights (M_W) of 2000 and 5000 g/mol and a polydispersity of 1.7, was purchased from Sigma Aldrich and used without further purification. To adsorb polyelectrolytes onto the surface of the nanoparticles, we have followed the precipitation−redispersion protocol, as described elsewhere.[24,29] This simple technique allowed production of large quantities of coated particles (> 1 g of oxides) within a relatively short time (< 1 h). The precipitation of the cationic cerium or iron oxide dispersion by PAA was performed under acidic conditions (pH 2). The precipitate was separated from the solution by centrifugation, and its pH was increased by addition of ammonium hydroxide. The precipitate redispersed spontaneously at pH 7−8, yielding a clear solution that now contained the polymer-coated particles. The hydrodynamic sizes of the PAA_{2K}−CeO_2, PAA_{2K}−γ-Fe_2O_3, and PAA_{5K}−γ-Fe_2O_3 dispersions were found to be 13, 19, and 22 nm, respectively. These values were 4−5 and 8 nm larger than the hydrodynamic diameter of the uncoated particles, indicating a corona thickness h of 2−2.5 nm for PAA_{2K} and 4 nm for PAA_{5K} (Table 2). In terms of coverage, the number of adsorbed chains per

(30) Lindner, P.; Zemb, T. *Neutrons, X-rays and Light: Scattering Methods Applied to Soft Condensed Matter*; Elsevier: Amsterdam, 2002.
(31) Dubois, E.; Cabuil, V.; Boue, F.; Perzynski, R. *J. Chem. Phys.* **1999**, *111* (15), 7147–7160.
(32) Dubois, E.; Perzynski, R.; Boué, F.; Cabuil, V. *Langmuir* **2000**, *16*, 5617–5625.
(33) Biggs, S.; Healy, T. W. *J. Chem. Soc., Faraday Trans.* **1994**, *90*, 3415–3421.
(34) Vermöhlen, K.; Lewandowski, H.; Narres, H.-D.; Koglin, E. *Colloids Surf., A* **2000**, *170*, 181–189.
(35) Si, S.; Kotal, A.; Mandal, T. K.; Giri, S.; Nakamura, H.; Kohara, T. *Chem. Mater.* **2004**, *16*(18), 3489–3496.

particle was estimated to be in the range of 50−70.[24,36] As for the citrate-coated particles, it was determined by electrokinetic measurements that the PAA coating resulted in strongly anionic charged interfaces.[24,25,37] Electrophoretic mobility values are listed as Supporting Information.

As a final step of the three procedures described above, the dispersions were all dialyzed against DI-water with the pH first adjusted to 8 (Spectra Por 2 dialysis membrane with a molecular mass cutoff of 12 kDa). At this pH, 90% of the carboxylate groups of the citrate and PAA coating were ionized. The schematic representations of the different coatings are illustrated in Figure 2. The suspension pH was adjusted with reagent-grade nitric acid (HNO_3) and with sodium or ammonium hydroxides. For the assessment of the stability with respect to ionic strength, sodium and ammonium chloride (NaCl and NH_4Cl, respectively, from Fluka) were used in the I_S range of 0−1 M.

3. Culture Medium. The particle stability was evaluated using a cell culture medium consisting of Dulbecco's modified Eagle's medium (DMEM, PAA Laboratories, GmbH), 10% fetal calf serum (FCS, PAA Laboratories, GmbH), 100 units/L penicillin, and 100 mg/L streptomycin (PAA Laboratories, GmbH). In its commercial formulation, DMEM also contained 4.5 g/L D-glucose, inorganic salts such as sodium chloride (6400 mg/L), sodium hydrogen carbonate (3700 mg/L), potassium and calcium chloride (400 and 200 mg/L, respectively), and 17 amino acids in different concentrations ranging from 50 to 1000 mg/L (e.g., L-glutamine). Vitamins such as myoinositol (7.2 mg/L) and folic acid (4 mg/L) were also present in the culture medium, however, in smaller amounts. Most of these additives were charged species and as a result increased the ionic strength (I_S) of the solution to 0.16 M.

4. Transmission Electron Microscopy. TEM experiments were conducted on a Jeol-100 CX microscope at the SIARE facility of the University Pierre et Marie Curie (Paris 6). The TEM images of the cerium and iron oxide nanoparticles were obtained at a magnification of 120000× (Figure 1), and their size distributions were derived using ImageJ (http://rsb.info.nih.gov/ij/). The diameter and polydispersity for CeO_2 were in good agreement with those determined by cryogenic transmission electron microscopy (cryo-TEM) in an earlier report.[25]

5. Static and Dynamic Light Scattering. Static and dynamic light scattering were performed on a Brookhaven spectrometer (BI-9000AT autocorrelator, λ = 632.8 nm) for measurements of the Rayleigh ratio $\mathcal{R}(\mathbf{q},c)$ and of the collective diffusion constant $D(c)$. The Rayleigh ratio was obtained from the scattered intensity $I(\mathbf{q},c)$ measured at the wavevector $\mathbf{q}$ according to the equation $\mathcal{R}(\mathbf{q},c) = \mathcal{R}_{std}[I(\mathbf{q},c) - I_S]/I_{Tol}$, where $\mathcal{R}_{std}$ is a standard Rayleigh ratio for toluene, I_S and I_{Tol} are the intensities measured for the solvent and for toluene, respectively, and $q = (4\pi n/\lambda)\sin(\theta/2)$ (n being the refractive index of the solution and θ the scattering angle). In this study, the suspending solvent was deionized water with or without added salt, or the DMEM-based cell culture medium. In the regime of weak colloidal interactions, the Rayleigh ratio $\mathcal{R}(\mathbf{q},c)$ is predicted to follow a wavevector and concentration dependence such as[30]

$$\frac{Kc}{\mathcal{R}(\mathbf{q},c)} = \frac{1}{M_{w,app}}\left(1+\frac{\mathbf{q}^2 {R_G}^2}{3}\right)+2A_2c \qquad (1)$$

In eq 1, $K = 4\pi^2 n^2 (dn/dc)^2/N_A\lambda^4$ is the scattering contrast coefficient (N_A is Avogadro's number), $M_{w,app}$ is the apparent molecular weight, and A_2 is the second virial coefficient. The concentrations targeted in this work were chosen so as to cover the concentration ranges classically investigated in toxicology assays. Expressed in molar concentrations of metallic atoms, these concentrations ([Ce] and [Fe]) ranged from 0.1 to 10 mM. Molar concentrations of 10 mM corresponded to cerium (resp. iron) oxide weight concentration of 0.17 wt % (resp. 0.08 wt %). In the dilute regime, $\mathbf{q}R_G \ll 1$ and $A_2 \sim 0$ in eq 1, which then reads

$$\mathcal{R}(\mathbf{q},c) = KM_{w,app}c \qquad (2)$$

This latter equation emphasizes the fact that for sub-10 nm particles, the Rayleigh ratio does not depend on the wavevector in the characteristic $\mathbf{q}$ window of light scattering. In this regime, the coated NP dispersions were found to obey eq 2. Table 2 summarizes the experimentally determined Rayleigh ratio increments $\mathcal{R}(c)/c$ for the seven systems considered here ($\theta = 90°$). In this work, the intensity scattered by nanoparticles dispersed in a cell growth medium was evaluated as a function of time and concentration. In the case of a destabilization of the sol, the scattering intensity was expected to grow above the predictions of eq 2. With an accuracy of better than 5%, this technique was very sensitive to the state of a dispersion. With light scattering operating in dynamical mode, the collective diffusion coefficient D was determined from the second-order autocorrelation function of the scattered light. From the value of the coefficient, the hydrodynamic diameter of the colloids was calculated according to the Stokes−Einstein relation $D_H = k_B T/3\pi\eta_S D$, where k_B is Boltzmann's constant, T the temperature (298 K), and η_0 the solvent viscosity ($\eta_S = 0.89 \times 10^{-3}$ Pa s for water and 0.95×10^{-3} Pa s for DMEM supplemented with calf serum and 25 °C).[38] The autocorrelation functions were interpreted using

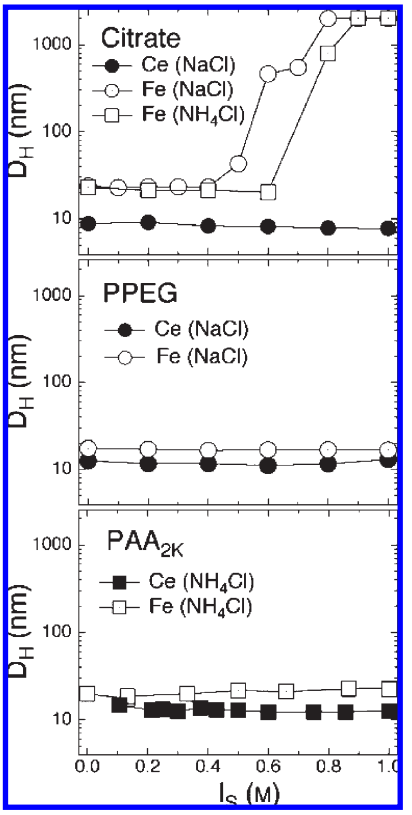

Figure 3. Hydrodynamic diameter for various inorganic nanoparticle dispersions [(filled symbols) cerium oxide and (empty symbols) iron oxide] as a function of ionic strength. I_S was adjusted using sodium (circles) and ammonium (squares) chloride. Except for Cit−γ-Fe_2O_3, all other dispersions were stable at ionic strengths up to 1 M.

(36) Fresnais, J.; Berret, J.-F.; Frka-Petesic, B.; Sandre, O.; Perzynski, R. *Adv. Mater.* **2008**, *20*(20), 3877–3881.
(37) Berret, J.-F. *Macromolecules* **2007**, *40*(12), 4260–4266.
(38) Gosgnach, W.; Messika-Zeitoun, D.; Gonzalez, W.; Philipe, M.; Michel, J. B. *Am. J. Physiol.* **2000**, *279*(6), C1880–C1888.

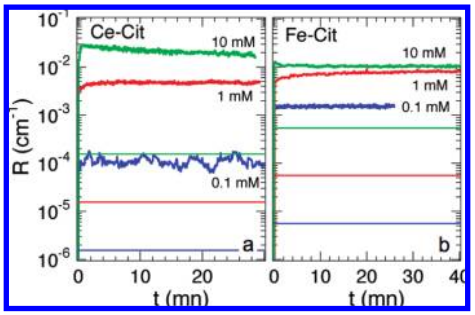

Figure 4. Time dependences of the Rayleigh ratio measured by static light scattering for Cit−CeO_2 (a) and Cit−γ-Fe_2O_3 (b) in DMEM supplemented with calf serum and antibiotics. The time at which nanoparticle dispersions were added to the culture medium provided the origin on the time axis. The concentrations investigated were taken so as to cover the concentration ranges investigated in toxicology assays. Expressed in molar concentrations of metallic atoms, these concentrations ([Ce] and [Fe]) ranged from 0.1 to 30 mM. The color code for Figures 4−8 is as follows: blue for 0.1 mM, red for 1 mM, green for 10 mM, and orange for 30 mM. The horizontal lines were calculated assuming that the particles remained in a dispersed state (from eq 2 and Table 2). The color code was the same as for the data. The large scattering excess between the experimental and calculated values was interpreted as the signature of the destabilization of the citrate-coated particles.

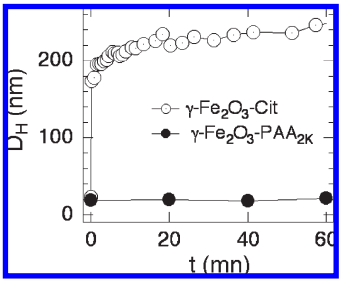

Figure 5. Time evolution of the hydrodynamic diameter of Cit−γ-Fe_2O_3 and PAA_{2K}−γ-Fe_2O_3 dispersions (1 mM Fe) in DMEM supplemented with calf serum and antibiotics. The steep increase in D_H at short times was interpreted as an indication of the destabilization of the dispersion. For the PAA_{2K}-coated particles, D_H remained constant over the duration of the experiment and over a time longer than weeks.

the cumulants and the CONTIN fitting procedure provided with the instrument software.

III. Results and Discussion

1. Effect of Salt. Applications of NPs in biology require that they be stable in solutions containing high concentrations of proteins and salts, as well as in cell culture media. The particles put under scrutiny in this work were first tested with respect to changes in concentration, pH, and ionic strength. With water as a solvent, stability was found up to a c of 10 wt % and for pH 5−11.[15] Note that PPEG-coated particles were stable over a broader range, from pH 1.5 to 10.[26] Here, we illustrate the behavior as a function of ionic strength I_S. The hydrodynamic diameters obtained by light scattering are displayed in Figure 3 for I_S values from 0 to 1 M. I_S was adjusted using sodium (circles) and ammonium (squares) chloride. Figure 3a shows that Cit−γ-Fe_2O_3 was destabilized by addition of both salts (at I_S = 0.45 M for NaCl and I_S = 0.65 M for NH_4Cl), whereas Cit−CeO_2 sustained ionic strength up to 1 M. The samples coated with pegylated oligomers (PPEG−CeO_2 and PPEG−γ-Fe_2O_3)

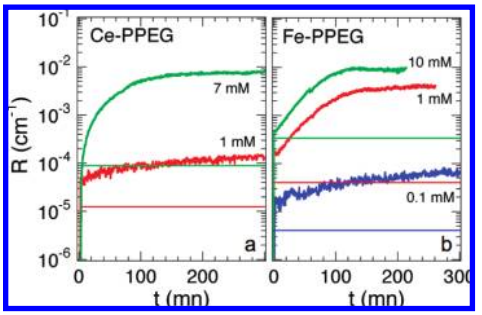

Figure 6. Same as Figure 4, but for PPEG−CeO_2 (a) and PPEG−γ-Fe_2O_3 (b) nanoparticles.

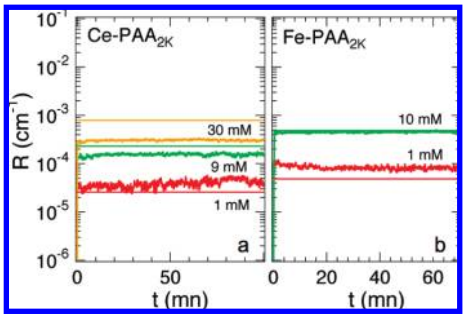

Figure 7. Same as Figure 4, but for PAA_{2K}−CeO_2 (a) and PAA_{2K}−γ-Fe_2O_3 (b) nanoparticles. The color code is as follows: red for 1 mM, green for 10 mM, and orange for 30 mM. The good agreement between experimental and calculated data was interpreted as an indication that the particles were stable in the cell culture medium.

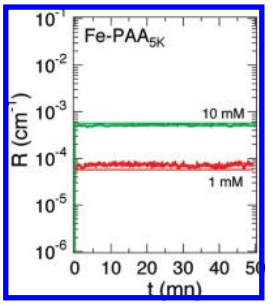

Figure 8. Same as Figure 4, but for PAA_{5K}−γ-Fe_2O_3 nanoparticles. The color code is as follows: red for 1 mM and green for 10 mM. The good agreement between the experimental and calculated results was interpreted as an indication of a superior stability in the cell culture medium.

and with ion-containing polymers (PAA_{2K}−CeO_2 and PAA_{2K}−γ-Fe_2O_3) were all stable up to an I_S of 1 M. We have recently exploited this feature to control the aggregation of magnetic particles and to design superparamagnetic nanorods.[36]

2. Stability in Cell Culture Medium. Panels a and b of Figure 4 show the time dependences of the Rayleigh ratio for the citrate-coated Cit−CeO_2 and Cit−γ-Fe_2O_3 NPs, respectively. In these experiments, a few microliters of concentrated NP dispersions were mixed with 1 mL of freshly prepared culture medium. The time at which the mixing was made provided the origin on the abscissa (Figure 4). As stated in the Experimental Section, the amount of added dispersion was calculated so as to cover molar concentrations [Ce] and [Fe] ranging from 0.1 to 10 mM. In the six experiments shown in Figure 4, the Rayleigh ratio remained constant, but at values which did not scale with concentration (as expected from eq 2). For Cit−CeO_2 at 10 mM Ce, a decrease in

Table 3. Hydrodynamic Diameters Measured for Coated Nanoceria under Three Different Solvent Conditions (in deionized water, in the cell culture medium after 1 day and after 1 week)

		D_H (nm)		
coated CeO_2	[Ce] (mM)	DI-water	culture medium for 1 day	culture medium for 1 week
Cit−CeO_2	0.1	10	36	nd[a]
	1		300	330[b]
	10		1150	740[b]
PPEG−CeO_2	0.1	12	20	21
	1		25	480
	7		400	300[b]
PAA_{2K}−CeO_2	1	13	18	nd[a]
	9		15	nd[a]
	30		13	14

[a] Not determined. [b] Dispersions that were diluted prior to the measurement to reduce absorption and multiple scattering.

Table 4. Same Data as in Table 3 for Coated Maghemite

		D_H (nm)		
coated γ-Fe_2O_3	[Fe] (mM)	DI-water	culture medium for 1 day	culture medium for 1 week
Cit−γ-Fe_2O_3	0.1	23	184	nd[a]
	1		220	200
	10		375	nd[a]
PPEG−γ-Fe_2O_3	0.1	17	220	nd[a]
	1		264	nd[a]
	8		2380	230[b]
PAA_{2K}−γ-Fe_2O_3	1	19	20	21
	10		18	19
PAA_{5K}−γ-Fe_2O_3	1	22	21	25
	10		20	23

[a] Not determined. [b] Dispersions that were diluted prior to the measurement to reduce absorption and multiple scattering.

the intensity was even observed over the first 30 min of the experiment. Further insights can be gained by comparing the levels of the scattering intensity with the predictions calculated from eq 2. These predictions were made using the results listed in Table 2 and assuming that (i) the particles remained in a dispersed state and (ii) the coupling constant K was identical in DI-water and in the culture medium. These estimations are the horizontal lines in Figure 4 with the same color code as for the data (blue for 0.1 mM, red for 1 mM, green for 10 mM, and orange for 30 mM). As a result, for Cit−CeO_2 and Cit−γ-Fe_2O_3, we have found that the actual scattering intensity was 10−1000-fold higher than that of dispersed particles. These findings are the signature that Cit−CeO_2 and Cit−γ-Fe_2O_3 NPs were destabilized at the contact of the culture medium. The destabilization was actually very rapid, and intermediate values of the scattering could not be recorded. These outcomes also confirmed the direct visual observations of test tubes that showed high turbidity with the addition of particles. The experiments depicted in Figure 4 were restricted to short periods (< 1 h), because at longer times the aggregates sedimented.

To demonstrate further the destabilization of the nanosols, the hydrodynamic diameter of the Cit−γ-Fe_2O_3 dispersions (1 mM Fe) was monitored as a function of the time over a period of 1 h (Figure 5). At the mixing, D_H exhibited a steep increase from its initial value of 23 nm to a value of ~170 nm. The diameter evolved further and showed saturation around 250 nm. The increase in D_H was also accompanied by a broadening of the size distribution. At longer times (> 1 h), the large aggregates sedimented, resulting in the reduction of both the scattering intensity and diameter. The data in Figure 5 are in excellent agreement with those of the time evolution of the Rayleigh ratios for the same samples, both quantities indicating destabilization of the particles.

Panels a and b of Figure 6 display the Rayleigh ratios for the pegylated cerium and iron oxide NPs, PPEG−CeO_2 and PPEG−γ-Fe_2O_3 respectively. Data for 1 and 7 mM cerium and from 0.1 to 10 mM iron oxide were collected over periods of 5 h. For the five samples investigated, the same qualitative behavior was reported. Soon after the addition of the particles to the cell medium, the scattering intensities were on the order of those calculated for the disperse state. This state lasted a few minutes, and then the Rayleigh ratios started to increase, to finally saturate at much higher values ($R = 10^{-2}$ cm^{-1} for the most concentrated specimens). As for the citrate-coated particles, the excess scattering at steady state was 1−2 decades above the single-particle predictions, indicating again a destabilization of the dispersions. As for the citrate-coated particles, this destabilization could be observed visually, since the suspending liquid became turbid after some time (more than hours).

As for the PAA_{2K}- and PAA_{5K}-coated NPs, the data in Figures 7 and 8 show a constant level of scattering after the introduction of the particles into the culture medium. This property was observed at all concentrations investigated, up to 30 mM Ce and 10 mM Fe. Moreover, the scattering levels were in good agreement with the predictions made for disperse solutions. The agreement was indeed excellent for the PAA_{2K}−CeO_2 dispersion at 1 mM Ce and for PAA_{2K}−γ-Fe_2O_3 and PAA_{5K}−γ-Fe_2O_3 dispersions 1 and 10 mM Fe. For the 30 mM Ce specimen, we even observed a scattering intensity that was lower than the computed value. One possible reason for this was that at this concentration, interparticular (repulsive) interactions took place and lowered the intensity at the wavevector of the experiment.[30] The remarkable stability of the PAA_{2K}-coated particles was further evidenced by the measurement of the hydrodynamic diameter as a function of time ([Fe] = 1 mM, bottom curve in Figure 5). There, D_H remains unchanged over the duration of the experiment.

For the assessment of the colloidal stability over longer periods, the hydrodynamic diameters were determined 1 day and 1 week after the mixing. Tables 3 and 4 list the D_H values for the 19 cerium and iron oxide dispersions. Three stability trends are particularly noteworthy here. (i) After a period of 1 week, the findings of Figures 4−8 were corroborated: the citrate- and PPEG-coated particles with D_H values between 200 and 740 nm were sedimented at the bottom of the test tubes. In contrast, the poly(acrylic acid)-coated particles were fully dispersed in the culture medium, with a D_H of 14 nm for PAA_{2K}−CeO_2 and a D_H of 19 nm for PAA_{2K}−γ-Fe_2O_3. (ii) The stability behavior of particles in the cell culture medium depended more strongly on the coating than on the nature of the particle or the concentration. Particles with the same coating behave similarly. (iii) When destabilization occurred, which is the case for the citrate- and PEG-coated particles, the cluster sizes also vary with the initial concentration. As illustrated by the Cit−CeO_2 specimen in Table 3, the higher the concentration, the larger the aggregates. This result is reminiscent of well-known mechanisms, such as the aggregation limited by the diffusion.[39] In summary, the most remarkable result obtained here was the excellent long-term stability of the PAA_{2K}- and PAA_{5K}-coated particles.

IV. Concluding Remarks

In this paper, we have shown that the coating plays an important role in the stability of aqueous dispersions of sub-10 nm cerium and iron oxide particles. Static and dynamic light

(39) Witten, T. A.; Sander, L. M. *Phys. Rev. Lett.* **1981**, *47*(19), 1400–1403.

scattering experiments were performed as a function of time, for times between 1 s and 1 week (10^6 s) after the introduction of particles into a conventional cell culture medium. A careful analysis of the data allows us to draw conclusions about the stabilization or destabilization mechanisms, as well as about the long-term fate of the inorganic particles in these specific environments.

According to DLVO theory, colloidal stability is ensured when steric and electrostatic interactions are able to counterbalance the short-range van der Waals attractive interactions.[40] Following this approach, the destabilization observed with the citrate- and PPEG-coated particles could arise from several mechanisms. A first mechanism would be related to the ionic strength gap that the particles bridge by switching from one solvent (DI-water; $I_S <$ 1 mM) to another (DMEM supplemented with calf serum; $I_S =$ 0.16 M). In this case, the range of electrostatic interactions diminished through the decrease in the Debye screening length (from 10 to 0.7 nm), resulting in the onset of an aggregation process. Another possible mechanism for the destabilization could be the desorption of the adlayer through a competitive exchange with other components present in the culture medium. These components would then be the amino acids in DMEM or the plasma proteins stemming from the calf serum. The multivalent counterions, such as calcium and magnesium present in DMEM, could also play a crucial role. Changing the type and amount of species at the liquid−solid interface has the consequence of modifying the range and ratio of the steric, electrostatic, and van der Waals interactions between particles and accelerating their uncontrolled clustering and final precipitation.

From the data shown in Figure 3 (D_H vs I_S), the citrate-coated particles were destabilized by the addition of salts, but for ionic strengths above 0.45 M with NaCl and 0.65 M with NH_4Cl, i.e., higher than that of the growth medium. Therefore, the screening of the electrostatic interactions occurring at the mixing might not be the relevant mechanism here. We have also found that the particles behave very similarly in DMEM and in DMEM supplemented with calf serum and antibiotics. We hence argue that the destabilization of the citrate- and PPEG-coated particles probably started by the desorption of the coating through exchange with components present in the solvent. This mechanism is very rapid for the case of citrate (< 1 s) and slower for the PPEG-coated particles (hours).

From the rationale given above, and with regard to the excellent stability of the PAA-coated particles, it can been deduced that the poly(acrylic acid) chains were strongly attached to the particle surfaces. As already documented by Seghal et al.,[24] we assume that this attachment occurred through the electrostatic adsorption of a few monomers (10−15 units for PAA_{2K})[24] with the cationic charges on the surfaces, the remaining part of the chain being stretched toward the solvent. The anionic adlayers confer to the particles both the steric and electrostatic repulsions of charged brushes.[41] The combination of these two attributes (yielding the term electrosteric for the this type of repulsion),[22] together with the multipoint attachment of the chain, is at the origin of the remarkable colloidal stability in high-ionic strength solvents and in cell culture media. As a final comment, it is important to notice that hydrodynamic diameters of the PAA-coated particles were not altered in the cell culture medium, even after 1 week, indicating that there was no protein adsorption on the electrosteric brushes. These findings finally suggest that low-molecular weight anionic polyelectrolytes represent a powerful alternative to conventional coating agents such as poly(ethylene oxide).

Acknowledgment. We thank Olivier Sandre, Bruno Frka-Petesic, Régine Perzynski, Cyrille Richard, Nathalie Mignet, Jean-Paul Chapel, Hiba Sarrouj, and Nathalie Luciani for numerous and fruitful discussions during the course of this work. The Laboratoire Physico-chimie des Electrolytes, Colloides et Sciences Analytiques, and the Rhodia rare earths team at the Centre de Recherche d'Aubervilliers (Aubervilliers, France) are acknowledged for providing us with the nanoparticle dispersions. This research was supported in part by Rhodia (France), by the Agence Nationale de la Recherche, under Contract BLAN07-3_206866, and by the European Community through the project "NANO3T—Biofunctionalized Metal and Magnetic Nanoparticles for Targeted Tumor Therapy", Project 214137 (FP7-NMP-2007-SMALL-1).

Supporting Information Available: Coating and coated nanoparticles (SI.1) and long-term stability of functional nanoparticles in cell culture medium (SI.2). This material is available free of charge via the Internet at http://pubs.acs.org.

(40) Israelachvili, J. N. *Intermolecular and Surfaces Forces*, 2nd ed.; Academic Press: New York, 1992.

(41) Groenewegen, W.; Egelhaaf, S. U.; Lapp, A.; Maarel, J. R. C. v. d. *Macromolecules* **2000**, *33*, 3283–3293.